
MODELING THE VAPORIZATION OF GEL FUEL DROPLETS

A. Kunin, B. Natan, and J. B. Greenberg

Experimental evidence of the combustion process of gel droplet burning indicates that, at a certain time after ignition, evaporation of the liquid fuel results in the formation of an elastic film of high viscosity gellant around the droplet that prevents further vaporization. As a result, constantly expanding vapor bubbles are produced within the droplet. Eventually, the film is ruptured and a jet of fuel vapor is released. A theoretical, time-dependent model of organic-gellant-based gel droplet combustion has been developed and numerically solved. The results indicate that the evaporation rate of the liquid fuel from the droplet surface and the viscosity of the components comprising the gel droplet affect the formation and modification of the gellant layer. The tensile stress, applied on the gellant film during the formation of the bubbles, reaches high levels in short periods of time and causes the droplet to rupture when it exceeds the layer material yield-point.

NOMENCLATURE

C	bubble formation parameter
c	molar concentration
D	diffusion coefficient
E_v	evaporation rate parameter
M	molecular weight
p	pressure
R	normalized external droplet radius
r	radial coordinate (normalized)
r_0	radius of gel droplet
T	temperature
t	time (normalized by r_0^2/D_{fg})
\tilde{V}	molar volume of the liquid
V_b	volume of the bubble
V_l	combined volume of the liquid fuel and the gellant
V_R	total volume of the droplet
X	normalized gellant layer thickness
Z	gellant content in gel

Greek Symbols

μ	viscosity
ρ	density
σ	tensile stress
σ_y	yield stress
Ψ_B	association parameter (Wilke correlation)

Subscripts

A, B	components
f	fuel
g	gellant
fg	liquid fuel/gellant mixture
l	liquid
v	evaporation

1 INTRODUCTION

There are two important parameters that have to be taken into account when considering the use of a propellant in various aerospace applications — energetic performance and safety features. Gel propellants are advantageous because they provide a promising response to both of these important requirements. In this particular liquid–solid state, these unique propellants combine the advantages of liquid and solid propellants.

Gel fuels are liquids whose rheological properties have been altered by the addition of gellants, so that they behave as non-Newtonian time-dependent fluids. The existence of yield stress and the increased viscosity can prevent agglomeration, aggregation, and separation of a metal solid phase from the fuel during storage. Their performance characteristics and operational capabilities, which are similar to liquid propellants, as well as their high density, increased combustion energy and long-term storage capability, make them attractive for many applications, especially for volume-limited propulsion system applications. An extensive review of various aspects of gel propellants was given by Natan and Rahimi [1].

In the present study, the attention is turned to recent experimental work conducted by Solomon and Natan [2, 3] on the combustion of organic-gellant-based fuels. They found that at the beginning of the burning process, an organic-gellant-based fuel droplet consists of a homogeneous, highly viscous liquid whose burning can be classified as “classic” liquid droplet combustion with a distinct

flame envelope that surrounds the droplet. In comparison with a liquid droplet, the turbulence intensity inside the droplet is low due to the high viscosity so that internal mixing is very slow. Due to the difference between the boiling point temperature and the heat of vaporization of the liquid fuel and the organic gellant, the homogeneity of the mixture cannot be maintained and the concentration of the liquid fuel at the outer part of the droplet decreases continuously. At some point, a film of very high viscosity gellant is formed around the droplet, enclosing the gel, and the result is that liquid fuel cannot pass through the gellant layer and evaporate towards the flame. Consequently, droplet heating results in the formation of fuel vapor bubbles inside the droplet. Expansion of the bubbles results in significant swelling of the droplet while the pressure inside the bubbles remains approximately constant. The thickness of the viscous gellant layer decreases as the droplet expands until the film is ruptured, and a jet of fuel vapor is released. The envelope collapses back onto the droplet and a new gellant layer is formed. This process repeats itself several times until the mostly gellant droplet burns out completely. This phenomenon is strikingly different from the widely accepted behavior of pure liquid-fuel droplets.

In general, gel fuels consist of Z percent of gellant that can be organic or inorganic and $(100 - Z)$ percent of liquid fuel (mostly kerosene-based, e.g., JP-5 and JP-8 fuels). The gellant itself consists of a blend of components including in most cases a liquid solvent (e.g., MIAK — Methyl Isoamyl Ketone) and the actual gellant, which is an organic material. The mass concentration of the gellant varies from 7.5% (as in [4]) to 15% (as in [3]). The advantage of organic over inorganic gellants is their ability to burn, whereas inorganic gellants are inert. Therefore, gel fuels can be regarded as multicomponent fuels with special and unique properties.

Extensive theoretical and experimental work was conducted in the field of multicomponent fuel droplet evaporation/burning. Law [5] analyzed isobaric, spherically symmetric combustion of a droplet with a spatially uniform (but varying with time) temperature and composition (Rapid Mixing Model). The theoretical results of Law indicated that participation in vaporization is dominated by the most volatile species in the droplet and the droplet temperature is quite close to the steady state boiling point (BP) temperature of that species. Sirignano [6] argued that the uniform temperature and concentration limit results from the infinite diffusivity limit, and the model should therefore be regarded as an Infinite Diffusivity Model. In other theoretical work, Tong and Sirignano [7] proposed another approach to the problem using a vortex model. This was basically a diffusion limit model that was previously formulated by Landis and Milles [8]. Based on these results, they concluded that the liquid phase mass diffusion is extremely slow and represents the rate limiting process. By analyzing transient multicomponent droplet combustion, Mawid and Aggarwal [9] determined that the concentration of the fuel vapor inside the flame may become higher than that at the droplet surface and as a result, suppression of the vapor-

ization process may happen. These effects occur most likely due to high liquid-phase mass diffusion resistance that prevents the more volatile component from diffusing rapidly to the droplet surface. Experimental work [10, 11] confirmed most of the theoretical results presented above. However, all the aforementioned work was concerned with ungelled liquid fuel droplets.

The aim of the present paper is to describe the peculiar phenomenon of the combustion process of a single organic-gellant-based gel fuel droplet in the framework of a theoretical time-dependent model. As a first step in establishing a physical model based upon the main mechanisms involved in the combustion of a gel droplet (as observed in experimental investigations), an often-adopted strategy of an order-of-magnitude analysis is implemented. This enables one to carry out a straightforward mathematical/numerical analysis that leads to a relatively easy formulation of the problem and its solution. In the ensuing sections, the assumptions underlying the model are explained, the model equations and the boundary conditions, as well as the method of solution are described, and in the final section, computed results that highlight the main characteristics of the organic-gellant-based gel fuel droplets combustion are discussed.

2 PROBLEM DESCRIPTION AND MATHEMATICAL MODEL

From the described experimental investigation on the combustion of an organic-gellant-based fuel droplet, the most fundamental elements can be extracted: at a certain time, a film of high viscosity gellant is created around the droplet that prevents further evaporation of liquid fuel. Consequently, a fuel vapor bubble is formed inside the droplet. The thickness of the viscous gellant layer decreases as the droplet expands until the film is ruptured producing a jet of fuel vapor. The envelope collapses back into the droplet and a new layer is formed. The process of gel droplet burning is illustrated in Fig. 1.

Spherical symmetry is considered for the gel droplet combustion. Although it is well known that kerosene consists of various components of different boiling point temperatures [12], for simplicity it is assumed that the gel fuel behaves as a bi-component mixture of gellant and pure liquid fuel. Moreover, the temperature within the droplet is assumed to be uniform and constant, equal to the boiling point of the more volatile component. The viscosity of the gellant is significantly higher than that of the liquid fuel. Although the viscosities of the components, especially of the gellant, decrease during the heating process, at the current stage, they are treated as constant.

By dividing the model into two stages, the physicochemical mechanisms involved in the burning process can be analyzed. During the first stage, fuel is consumed and an all-gellant layer is formed, as presented in Fig. 1*a*. The modi-

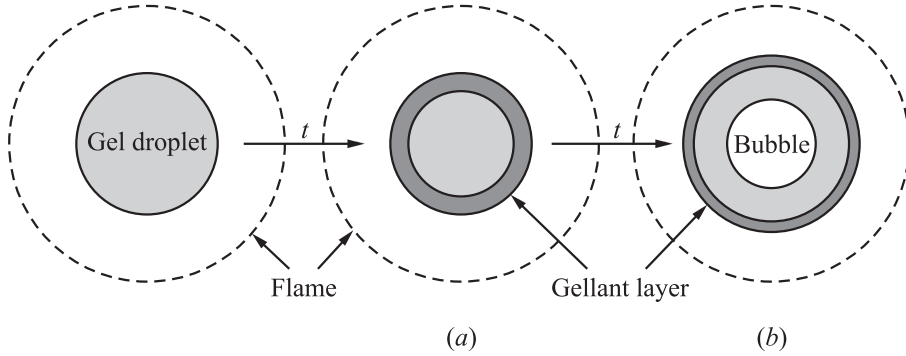


Figure 1 Schematic of gel droplet burning: (a) Stage 1 and (b) Stage 2

fication of the layer thickness with time occurs due to several contributions such as liquid diffusion in the gel droplet interior and vaporization through the layer. At the second stage, a bubble is formed. As a result, the droplet expands and the layer thickness decreases until it ruptures (Fig. 1b) when the tensile stress reaches the layer's yield point.

It is important to note that the mathematical formulation of the two stages concentrates mainly on internal droplet behavior. It is assumed that the flame that surrounds the gel droplet produces a sufficient heat flux to vaporize the liquid fuel during the first stage, and to enable formation of the vapor bubble in the droplet interior during the second stage. In this way, the various processes happening in the exterior to the droplet are not considered in the model development and only what is happening inside the gel droplet is investigated. A more comprehensive model of the entire burning process including the gel droplet surface — flame interaction — is also possible at the expense of further complexity. This will be formulated in future work.

Model of the First Stage

The physical model of the first stage is described schematically in Fig. 1a. The boiling point temperature of kerosene-based fuel ranges from 130 to 270 °C whereas the boiling point of the gellant ranges within 290–320 °C. This is the principal reason for the actual formation of the gellant layer around the droplet. In addition, there is very low, even no, internal circulation because of the high viscosity of the mixture. Consequently, a monotonic decrease of the liquid fuel from the outer surface of the fuel droplet occurs as the combustion process begins. As a result, diffusion of liquid fuel from the interior of the droplet towards the surface occurs. Saitoh and Nagano [13] also adopted this approach.

In general, gels behave as non-Newtonian fluids and “gel” is defined by Brinker and Scherer [14] as “a substance that contains a continuous solid skeleton

enclosing a continuous liquid phase. The continuity of the solid structure gives elasticity to the gel.” This is true when low (room) temperatures are considered. When the temperature of the gel mixture rises to relatively high values, such as the boiling point of liquid fuel, this unique structure does not exist anymore and the mixture can be treated as a bi-component liquid mixture with various diverse properties.

The mass diffusivity coefficient of a binary liquid mixture strongly depends on temperature, pressure and mixture composition. For the estimation of this coefficient, the empirical correlation proposed in [15, 16] is used:

$$D_{AB} = 7.4 \cdot 10^{-8} \frac{(\Psi_B M_B)^{1/2} T}{\mu \tilde{V}_A^{0.6}}. \quad (1)$$

The empirical relation that Eyring and his co-workers [17] developed for the variation of the viscosity with composition is described by:

$$\log \mu_{fg} = c_f \log \mu_f + c_g \log \mu_g.$$

The last expression can be rewritten in the following, more convenient way:

$$\mu_{fg} = \mu_f^{c_f} \mu_g^{c_g}.$$

So that the diffusion coefficient shown in Eq. (1) becomes:

$$D_{fg}(c_f) = \frac{K_{fg}}{\mu_f^{c_f(r,t)} \mu_g^{c_g(r,t)}}$$

where

$$K_{fg} = 7.4 \cdot 10^{-8} \frac{(\Psi_B M_B)^{1/2} T}{\tilde{V}_A^{0.6}}.$$

The general, nondimensional, nonlinear, time-dependent diffusion equation in a spherically-symmetric coordinate system for a bi-component mixture is:

$$\frac{\partial c_f}{\partial t} = \frac{1}{r^2} \frac{\partial}{\partial r} \left[D_{fg}(c_f) r^2 \frac{\partial c_f}{\partial r} \right].$$

In this equation, r represents the nondimensional radius coordinate and t represents nondimensional time, the latter being based on $t_{\text{diff}} = r_0^2 / K_{fg}$, where r_0 is the actual droplet radius. It is important to note that the last equation is valid for estimating the time variation of both molar concentrations (liquid fuel and gellant) along the droplet radius.

The initial and boundary conditions are:

$$\begin{aligned} t = 0: & \quad c_f = c_{f0} & \quad \text{at } 0 \leq r \leq 1; \\ t > 0: & \quad \begin{cases} \frac{\partial c_f}{\partial r} = 0 & \text{at } r = 0; \\ c_f = c_{f0} \exp(-E_v t) & \text{at } r = 1. \end{cases} \end{aligned}$$

The first initial condition gives the molar concentration of the liquid fuel at the beginning of the burning process; since the total molar concentration is equal to unity, the gellant concentration is $c_{g0} = 1 - c_{f0}$. The second boundary condition represents the symmetry at $r = 0$ and the last condition states that the decrease of liquid fuel molar concentration at the surface is described by an exponential function. E_v is a parameter that depends on different factors such as temperature, pressure, heat transfer, and others. Large E_v represents a high evaporation rate and a fast reduction of fuel concentration from the droplet surface, whereas low E_v represents a low evaporation rate and a slow reduction of liquid fuel from the surface.

The last boundary condition emphasizes again the strategy of isolating the field exterior to the droplet in the current model whilst concentrating on the droplet interior only. The actual estimation of the modification of layer thickness is determined by the points for which the composition of the layer reaches 90% gellant.

Model of the Second Stage

The physical model of the second stage is described schematically in Fig. 1b. The formation of a gellant layer with a defined thickness characterizes the termination of the first stage. This gellant layer prevents liquid fuel from penetrating through and evaporating toward the flame front. As a result, the formation of a vapor bubble in the interior of the droplet begins. Therefore, as the droplet expands, the layer thickness decreases until it ruptures when the tensile stress reaches the yield point of the material. This phenomenological description of gel droplet evaporation is based on the experimental study [2] described in the previous section. The gellant consists of 50% solvent and the remaining 50% is the actual gellant. The boiling point of the solvent (MIAK's BP temperature is 144 °C) is close to the BP of liquid fuel, therefore, they both evaporate simultaneously. The evaporation of the solvent from droplet surface results in phase separation, which in combination with the relatively low internal mixing, enhances the formation of the gellant layer.

The total volume of the gel droplet, $V_R(t)$, consists of the volume of the vapor bubble, $V_b(t)$, that is formed in the droplet interior and the remaining liquid mixture volume, $V_l(t)$:

$$V_b(t) + V_l(t) = V_R(t); \quad (2)$$

$$V_l(t) = V_{\text{initial},l} - \frac{\rho_{\text{vapor},b}}{\rho_l} V_b(t). \quad (3)$$

By combining Eqs. (2) and (3), the following expression for the evolution of total droplet volume is obtained:

$$V_b(t) \left\{ 1 - \frac{\rho_{\text{vapor},b}}{\rho_l} \right\} + V_{\text{initial},l} = V_R(t). \quad (4)$$

In order to approximate the density ratio (fuel vapor to liquid fuel) the thermodynamical data at 20 °C and 1 atm were chosen for demonstration. The density of liquid fuels is $\rho_l \approx 860\text{--}890 \text{ kg/m}^3$. Their vapor density is approximately $\rho_{\text{vapor},b} \approx 3.15 \pm 4.17 \text{ kg/m}^3$.

Consequently, from these data it can be easily concluded that the change in the liquid interior volume is minor in comparison to the change in the vapor volume.

Substituting these data in Eq. (4) gives the following expression for modification of the total droplet radius during the second stage:

$$R^3(t) = \frac{199}{200} r_b^3(t) + r_l^3.$$

Let $r_b(t) = f(t)$.

The growth of the vapor bubble in the droplet interior depends on a variety of factors such as the heat flux to the droplet, temperature, and pressure. As a first approximation, the bubble radius is assumed to change linearly with time. The constant of proportionality strongly depends on the various aforementioned parameters:

$$f(t) = Ct. \tag{5}$$

A large value of C represents quick growth of the vapor bubble — strong heat flux to the droplet. Low C represents slow growth of the vapor bubble — relatively low heat flux to the droplet.

Based on these assumptions, the gellant layer thickness during the second stage:

$$X(t) = \frac{r_l^2 X_{\text{initial}}}{R(t)^2}.$$

The question at this point is: When does the organic gellant layer rupture? To answer this question, the expression for the tensile stress applied to the thin layer sphere is described by:

$$\sigma(t) = \frac{R(t)p}{2X(t)}.$$

Obviously, when the tensile stress reaches the yield point of the material, the gellant layer is ruptured. In general, yield stress, $\sigma_y = \sigma_y(c_g, T)$, decreases with increasing temperature and decreasing gellant concentration. Evaluation of the actual values of yield stress will be estimated experimentally in the near future. Meanwhile, in the present work, the previous development is completed by formulating the normalized tensile stress (normalized by p , which is the vapor pressure in the bubble):

$$\tilde{\sigma}(t) = \frac{R(t)^3}{2r_l^2 X_{\text{initial}}}.$$

3 SOLUTION

The solution domain is essentially divided into two stages. At the first stage, the formation of the gellant layer is obtained by solving the diffusion equation with appropriate initial and boundary conditions. This nonlinear parabolic equation is solved numerically using a standard finite difference method. Satisfactory step sizes in the r and t directions were obtained by comparing computed results using a series of increasingly refined finite difference meshes to cover the region of the solution. At the second stage, the data gained from the first stage concerning the gellant layer thickness are substituted in appropriate expressions developed for the evaluation of the second stage.

For all cases, the following data were used: initial molar concentrations of the liquid fuel and of the gellant are $c_{f0} = 0.7$, $c_{g0} = 0.3$, respectively, liquid viscosity, $\mu_f = 100$ cP and gellant viscosity, $\mu_g = 10,000$ cP. The initial normalized thickness of the gellant layer is assumed to be $X_{\text{initial}} = 0.1$.

4 RESULTS

In the ensuing discussion, the numerical results obtained from both stages of the gel-droplet combustion model are presented. Note that all the parameters appear in nondimensional form.

The change, with time, of the molar concentrations of both components comprising the gel droplet (the liquid fuel and the organic-gellant in the interior of the droplet) is presented in Fig. 2. As mentioned, E_v is a parameter, which describes the rate at which liquid fuel evaporates from the droplet surface. For the current case, it is taken to be 1000, which represents a very high rate of liquid fuel evaporation.

In general, as expected, since the liquid fuel BP is lower than that of the gellant, the liquid fuel evaporates first, reducing its concentration while the gellant concentration increases.

The modification of the gellant layer thickness with time is presented in Fig. 3. The actual estimation of the layer thickness growth is determined by the points for which the composition of the gellant layer reaches 90%. For a high evaporation rate, the growth of the layer thickness is much faster in comparison to the case that corresponds to a low evaporation rate.

In Fig. 4, the influence of various viscosity-values of both components of the gel droplet (liquid fuel and gellant) on the modification of the gellant layer thickness is investigated. On the one hand, for sufficiently high mixture viscosities such as $\mu_g = 10,000$ cP; $\mu_f = 100$ cP, the diffusion coefficient obtained is significantly low; consequently, the rate at which the modification of the layer occurs will be also low. On the other hand, when the viscosities of both components

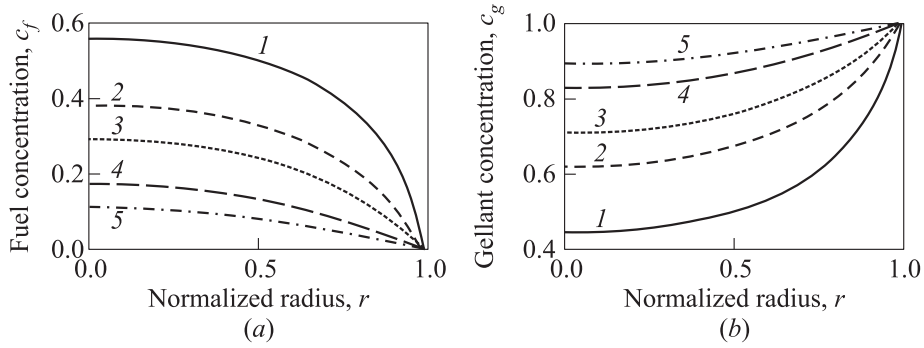


Figure 2 Fuel and gellant concentration in droplet interior; $E_v = 1000$, $\mu_g = 10,000$ cP, $\mu_f = 100$ cP: 1 — $t = 0.2$; 2 — 0.6; 3 — 1; 4 — 2; and 5 — $t = 3$

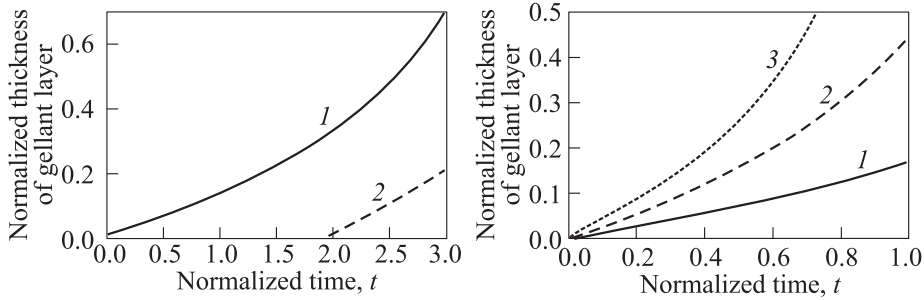


Figure 3 Gellant layer thickness evolution with time (Stage 1): 1 — $E_v = 1000$ and 2 — $E_v = 1$

Figure 4 Gellant layer thickness modification with time (Stage 1), $E_v = 1000$: 1 — $\mu_g = 10,000$ cP and $\mu_f = 100$ cP; 2 — $\mu_g = 1000$ cP and $\mu_f = 50$ cP; and 3 — $\mu_g = 100$ cP and $\mu_f = 10$ cP

are relatively low (i.e., $\mu_g = 100$ cP; $\mu_f = 10$ cP), the diffusion coefficient attains a higher magnitude, the gellant layer modification with time occurs at very high rates and it reaches a much bigger thickness. In comparison to the former case, almost three times more liquid fuel will evaporate prior to the layer formation in this case. Obviously, for a mean case, e.g., $\mu_g = 1000$ cP; $\mu_f = 50$ cP, the modification of the layer thickness lies in between the previously discussed boundaries.

During Stage 2, the bubble growth in the droplet interior is simulated by Eq. (5), and the parameter C is taken to be 0.1, 0.5, 1, and 2. In Fig. 5, the normalized gellant layer thickness as time goes by, for different rates of vapor

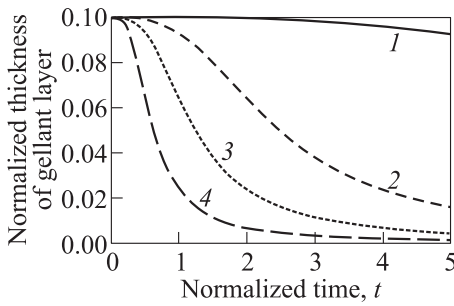


Figure 5 Gellant layer thickness evolution with time (Second stage): 1 — $C = 0.1$; 2 — 0.5 ; 3 — 1 ; and 4 — $C = 2$

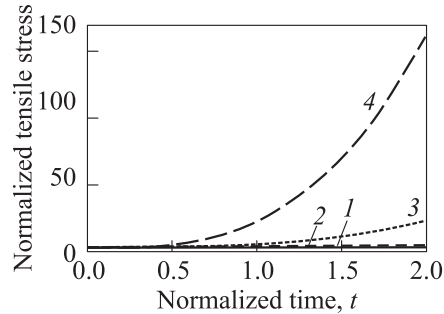


Figure 6 Tensile stress evolution with time: 1 — $C = 0.1$; 2 — 0.5 ; 3 — 1 ; and 4 — $C = 2$

bubble growth is presented. For very slow growth of the vapor bubble, the decrease in gellant layer is also slow whereas in the case of relatively high bubble growth, the layer thickness decreases drastically.

In addition, in Fig. 6, the variation of the tensile stress on the gellant layer is presented. A large value of tensile stress is reached in a relatively short period of time for the case of the rapidly growing bubble, $C = 2$.

5 CONCLUDING REMARKS

The baselines of a theoretical model describing the phenomena involved in the combustion of organic-gellant-based gel droplets have been presented for the first time. According to experimental investigation, during the burning of organic-gellant-based gels, an elastic layer made of gellant is formed around the droplet, resulting in periodic swelling, jetting, and collapsing of the droplet. This burning process of gel droplets is totally different from the burning of pure liquid fuel droplets and it repeats itself until all combustible material is consumed. By choosing rather simple mathematical functions, the rather complicated processes of gellant layer modification during its burning are reproduced. The results demonstrated the profound importance of the liquid fuel evaporation rate and of the viscosities of both components comprising the gel droplet, in the process of formation of the gellant film. Tensile stress, applied on the gellant film during the formation of the bubble in the droplet interior reaches high magnitudes in short periods of time and causes the droplet to rupture as soon as it overtakes the yield point of the layer material.

REFERENCES

1. Natan, B., and S. Rahimi. 2002. The status of gel propellants in year 2000. In: *Combustion of energetic materials*. Eds. K.K. Kuo and L. DeLuca. N.Y.: Begel House. 172–94.
2. Solomon, Y., and B. Natan. 2006. Experimental investigation of the organic gellant-based gel fuel droplets. *Combust. Sci. Technol.* 178(6):1185–99.
3. Solomon, Y., and B. Natan. 2006. Combustion of gel fuels based on organic gellants. AIAA Paper No. 2006-4565.
4. Von Kampen, J., F. Alberio, and H.K. Ciezki. 2007. Spray and combustion characteristics of aluminized gelled fuels with an impinging jet injector. *Aerospace Sci. Technol.* 11(1):77–83.
5. Law, C.K. 1976. Multicomponent droplet combustion with rapid internal mixing. *Combust. Flame* 26:219–33.
6. Sirignano, W. A. 1978. Theory of multi-component fuel droplet vaporization. *Arch. Thermodyn. Combust.* 9(2):231–47.
7. Tong, A. Y., and W. A. Sirignano. 1986. Multicomponent droplet vaporization in a high temperature gas. *Combust. Flame* 66(3):221–35.
8. Landis, R.B., and A.F. Milles. 1974. Effect of internal diffusional resistance on the evaporation of binary droplets. *5th Heat Transfer Conference (International) Proceedings*. Tokyo, Japan. B7-9:345–49.
9. Mawid, M., and S.K. Aggarwal. 1991. Analysis of transient combustion of a multicomponent liquid fuel droplet. *Combust. Flame* 84(1–2):197–209.
10. Wang, C.H., X.Q. Liu, and C.K. Law. 1984. Combustion and microexplosion of freely falling multicomponent droplets. *Combust. Flame* 56(2):175–97.
11. Wang, C.H., and C.K. Law. 1985. Microexplosion of fuel droplets under high pressure. *Combust. Flame* 59(1):53–62.
12. Edwards, T. 2002. Kerosene fuels for aerospace propulsion. AIAA Paper No. 2002-3874.
13. Saitoh, T., and O. Nagano. 1980. Transient combustion of a fuel droplet with finite rate of chemical reaction. *Combust. Sci. Technol.* 22(5–6):227–34.
14. Brinker, C.J., and G.W. Scherer. 1990. *Sol-gel science*. Boston: Academic Press, Inc.
15. Wilke, C.R. 1949. Estimation of liquid diffusion coefficients. *Chem. Eng. Progr.* 45:218–24.
16. Wilke, C.R., and P. Chang. 1955. Correlation of diffusion coefficients in dilute solutions. *AIChE J.* 1(2):264–70.
17. Glasstone, S., K.J. Laidler, and H. Eyring. 1941. *Theory of rate processes*. N.Y.: McGraw-Hill. Ch. 9.